Tunability of qubit Coulomb interaction: Numerical analysis of top-gate depletion in two-dimensional electron systems

A. Weichselbaum and S. E. Ulloa
Department of Physics and Astronomy, Nanoscale and Quantum Phenomena Institute, Ohio University, Athens, Ohio 45701, USA
(Received 27 April 2006; published 25 August 2006)

We investigate the tunability of electrostatic coupling between solid-state quantum dots as building blocks for quantum bits. Specifically, our analysis is based upon two-dimensional electron gas (2DEG) systems and depletion by top gates. We are interested in whether the Coulomb interaction between qubits can be tuned by electrical means using screening effects. The systems under investigation are analyzed numerically solving the Poisson equation in 3D via relaxation techniques with optimized algorithms for an extended set of boundary conditions. These include an open outer boundary, simulation of 2DEG systems, and dielectric boundaries like the surface of a physical sample. The results show that for currently lithographically available feature sizes, the Coulomb interaction between the quantum bits is weak in general due to efficient screening in the planar geometry of 2DEG and top gates. The evaluated values are on the order of 1 μeV. Moreover, while it is not possible to turn off the qubit interaction completely, an effective tunability on the order of 50% is clearly realizable while maintaining an intact quantum bit structure.

DOI: 10.1103/PhysRevB.74.085318 PACS number(s): 85.35.Be, 03.67.Lx, 85.35.Gv

I. INTRODUCTION

Quantum dot structures based upon localized regions of charge play an important role in investigating quantum-mechanical effects at the nanoscale.[1–3] Despite the short decoherence times, considerable progress is made in utilizing the charge degree of freedom for coherent quantum processes with possible application in quantum information.[4–6] In particular, electrostatically defined quantum dots, based on depletion of two-dimensional electron gas (2DEG) systems, play an important role due to their variability, as the charge "drop" in the dot can be controlled in shape and size by applying well-controlled gate voltages.

In this paper we consider a linear array of double dots as shown in Fig. 1. With different arrangements of voltage gates, quantum dots are formed and arranged in pairs to define charge qubits. Every pair is defined with a tunnel contact [quantum point contact (QPC)] between the two dots, which can be tuned by an external gate voltage. With the QPC in a weakly transparent regime, the charges are well localized in their respective quantum dot and the dot occupation is characterized by a well-defined number of electrons. The system can then be tuned to the energetically degenerate case, where an extra electron can reside on either quantum dot symmetrically. The dynamics of such a system is well described by the two qubit states $|L\rangle$ and $|R\rangle$, with the extra electron either on the left (L) or on the right (R) dot. These two states form the natural basis to define the two charge qubit configurations easily controlled by the gates that define the quantum dots and the QPC.[7]

As different dot pairs are used to define charge qubits via local gate voltages, their states are well defined and controlled experimentally. However, it is crucial to be able to control the interactions between neighboring qubits if one is to implement the quantum gate operations required in quantum computation.[8] We are thus interested here in the energetics of different charge configurations in the double-dot array and the *tunability* of the coupling between charge qubits via purely electrostatic means. Notice that including the interaction with neighboring qubits results in an effective dipole-dipole interaction (the common ZZ interaction in solid-state qubits in a spin notation). This causes the states in the qubit to align according to their neighbors and misalignments to be energetically costly. We investigate the energetics of different qubit configurations and how one can stabilize different states by purely electrostatic means.

For typical nanoscopic devices with many (or at least a few) electrons in each of the electrostatically defined regions, the charge distribution and the major energy scales are described to a good approximation by classical electrostatics.[9] Due to the strong electric fields generated by segregating charge in a 2DEG, the Coulomb energy is the dominant energy scale. Thus, it is important to know the electrostatics of the system if one expects a good quantitative description thereof. We present here a detailed study of the electrostatic coupling in the quantum dot array of Fig. 1. We find that one can substantially modify the qubit couplings by proper gate geometry and voltage control ($\approx$50%). However, we also find that it is not possible to completely turn off the coupling among dots, as one would need in order to allow for total decoupling of the system. Our studies utilize an efficient three-dimensional electrostatic code that uses higher-order grid relaxation and fast Fourier transform algorithms. This allows for accurate and realistic modeling of the quantum dot array of interest here, as well as a variety of other structures. Effects such as depletion in a 2DEG due to shallow etch[10] or deep etch[11] have been investigated with our code, and the results agree well with experimental data and other simulations built on Schrödinger Poisson solvers.[12]

FIG. 1. Linear array of double quantum dots. Charge is exchanged between the dots in each pair but different pairs are only coupled electrostatically. Defining gates are not shown.

As we mentioned above, we are interested in the tunability of the coupling between charge qubits. Electrostatically, tunability is directly related to changes in the geometry of the system—i.e., the regions were there is charge—since a constant geometry of electrically isolated regions implies a constant capacitance matrix and constant electrostatic coupling. Application of gate voltages produces changes in the lateral charge depletion on the 2DEG system, drastically changing the electric field line distribution around the area of interest. In the quantum dot structures analyzed here, this includes field lines that emerge out of the dots through the surface, as well as throughout the semiconducting material including the depleted 2DEG region. Notice, however, that depletion of charge in the 2DEG already suggests that the local electric field is strong with dominant field lines vertical to the 2DEG layer. Small local changes of charge or rearrangements are likely *not* to affect the interdot coupling strongly. This conclusion is not trivially reached, due to the complexity of the dot array and gate geometry, which includes subtle screening effects. Still, this intuitive picture turns out to be correct, as will be demonstrated in detail in the following.

II. SIMULATION OF 2DEG

2DEG systems are "volatile" by design; i.e., the electric charge can be depleted or accumulated by external means using appropriately fabricated conducting leads acting as voltage gates. Thus the 2DEG regions containing electric charge density change dynamically with the voltage patterns applied to the gates. For a flexible and reliable numerical analysis it is thus necessary that the 2DEG boundary be treated dynamically. The plane of the 2DEG may contain several independent regions of charge that can be addressed individually. Moreover, well-isolated regions of charge have a floating potential, and this situation remains even if weak tunnel junctions are present because of charge quantization. These considerations introduce a set of specific boundary conditions related to 2DEG systems. They are readily realized in our numerical code and explained in detail in Ref. 13. Moreover, as from a numerical point of view we are dealing with a finite system, the potential on the outer boundary floats freely and the system must be solved self-consistently. For more detail in that respect the reader is also referred to the Appendix .

The primary boundary condition for the 2DEG as it turns out is a surprisingly simple local update prescription built in easily with the relaxation sweeps:[13] when coming across a 2DEG grid point—say, point i—with the 2DEG layer kept from the exterior at the potential $V_{2\mathrm{DEG}}$, then proceed as follows: First, update the potential V_i locally as in homogeneous space. Second, if $V_i^{\mathrm{new}} > V_{2\mathrm{DEG}}$, take $V_i = V_{2\mathrm{DEG}}$; otherwise, accept the calculated V_i^{new}. The result is that the regions where $V_i = V_{2\mathrm{DEG}}$ contain electronic charge while the regions in the 2DEG with $V_i < V_{2\mathrm{DEG}}$ are depleted. The basic idea underlying this prescription is simply that for the electronic charges $q_i < 0$ in the 2DEG it is energetically favorable to go to a potential that is higher then $V_{2\mathrm{DEG}}$. The effect is that charges gather in these regions until the potential equilibrates at $V_{2\mathrm{DEG}}$.

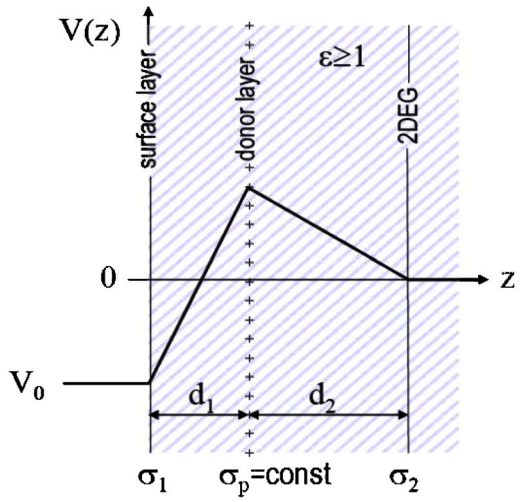

FIG. 2. (Color online) Electric potential $V(z)$ in a parallel plate geometry to demonstrate depletion in 2DEG—the material below the surface (to the right of the σ_1 layer) is considered uniform with a dielectric constant of ε. The charge densities on the three planes shown are σ_1, σ_p (p for the *positive* charge of the donor layer), and σ_2, respectively. V_0 is the total potential difference across the whole stack related to the pinning of the Fermi level at the surface.

The gross features of the charge distribution in a realistic sample with a uniform 2DEG system buried in close vicinity to the surface can be well understood by a parallel plate capacitor arrangement as shown in Fig. 2. σ_1 is the charge density at the free surface. A distance d_1 below lies the donor layer ("δ doping") with a doping density $\sigma_p \equiv en_D$, followed by the 2DEG separated by a distance d_2 from the donors. The variables d_1 and d_2 are parameters that can be adjusted to account for the finite width of each of the three layers. The electrical voltage V_0 of the surface with respect to the 2DEG is fixed as a consequence of the pinning of the Fermi energy at the surface and makes up for the difference in chemical potential due to surface states. For the case of Ga(Al)As, for example, the Fermi level is pinned to midgap,[14] and so the potential V_0 is chosen to be fixed at $V_0 \simeq -0.7$ V (note that the 2DEG is considered grounded).

The charges at the surface and in the 2DEG rearrange and equilibrate when the temperature is high enough, typically at room temperature. This leads to the energetically most favorable charge distribution that shares the charges available from the donor layer between the surface and the 2DEG such, that the electrical field above the surface and below the 2DEG of the sample is zero. The remaining adjustable parameter in a real system is then the distance d_1 which can be reduced by etching. The critical distance d_1^* for depletion of the 2DEG layer below is given by $d_1^{crit} = -V_0 \varepsilon \varepsilon_0 / en_D$ which is independent of the distance d_2 (note that V_0 is negative here).

With clearly separated layers of uniform charge, this capacitor model can be expected to provide a good description of charge distribution. The quantum-mechanical effects are implicitly present in the effective parameters d_1 and d_2 as well as in effects such as the pinning of the Fermi energy at the surface. To this extent, this semiclassical description of the system provides an accurate picture.[9]

III. ENERGETICS OF DOUBLE-DOT QUBITS

Double-dot systems are created in the 2DEG via depletion through negatively biased metallic top gates on the surface of the structure—e.g., fabricated by lithographic means. The typical system analyzed here is shown together with its numerical results in Fig. 3. The relatively large number of gates defining the structure keeps the system flexible. However, the exact number of gates and their respective arrangement are arbitrary to a certain extent and may be simplified by fewer gates in a specific experimental setup.

Every double-dot system (qubit) in our design has altogether six gates defining the dots, including a plunger gate for every dot, and two gates that tune the tunnel barrier (QPC) between the two dots defining the qubit. One of the two QPC gates for a pair of dots may eventually be merged with one of the gates confining the dot.

The set of top gates chosen can be seen in panel (a) of Fig. 3. The charge distribution shown with biased gates clearly outlines their geometry. The red shading (negative charge density) results from the negative bias voltages applied. Thus the more negative the bias, the larger the accumulated negative charge on that gate.

The potentials on the top gates were chosen as follows depending on the local degree of depletion that was required: −2.5 V on the plunger gates for every dot, −5.2 V for the QPC between a pair of dots, and −2.4 V for the transition region between pairs of quantum dots, except for the center transition whose gate potential was alternatively also set to 0 V. For the other confining potentials a value of −4.5 V was taken. The remaining (geometrical) parameters are pinning of the surface potential $V_0=-0.75$ V, dielectric constant $\epsilon=12$, grid spacing $h=12$ nm, $d_1=d_2=36$ nm, and $n_D=4\times10^{16}$ m^{-2}, resulting in a charge distribution ratio between the surface and the 2DEG of about 2:1.

In the setup of Fig. 3, the quantum dots contain about 200 electrons. In the following, the two adjacent qubits in the center of Fig. 3 are considered in more detail and the outer qubits allow us to examine the effect of qubit pair interaction. The plunger gate for individual dots was fine-tuned self-consistently at the end of the initialization process to produce half-integer occupancy on the dot. With this it is then an easy numerical task to achieve equivalent integer charge distributions for a single qubit with one extra electron symmetrically on either of the dots forming the qubit labeled as the two qubit states $|L\rangle$ and $|R\rangle$. More specifically, with the gate voltages frozen to their initial configuration for half-integer occupation of the dots, the charge configuration can now be altered to the possible different integer value charge configurations, shifting half of an electron in a quantum dot to the other or vice versa.

As indicated in Fig. 3, the gate in the center is introduced for the purpose of screening the qubit-qubit interaction through depletion or accumulation of charge in between the qubits, thus introducing the change of geometry of the charged regions necessary for tunability of the qubit interaction. The two resulting configurations analyzed are shown in panels (b) and (c) for the gate voltages $V_c=-2.4$ V and $V_c=0$ V, respectively. For the setup in panel (b), the different qubit states resulting from single-electron hopping on the two qubits in the center are presented in the panel (d). For better visual contrast, the difference in the charge configuration $\Delta q(\vec{r})$ in the layer of the 2DEG with respect to the initial half-integer setup is shown. When summing up $\Delta q(\vec{r})$ over a

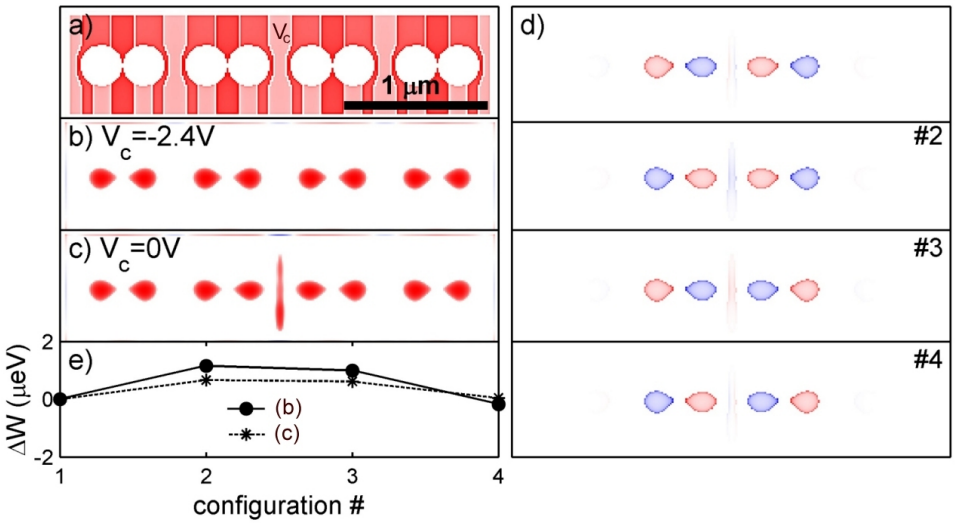

FIG. 3. (Color online) Simulation of 2DEG with top gates and applied gate voltages. The center gates [labeled V_c in panel (a)] extend in between the qubit pair such that the 2DEG underneath the gate V_c can be depleted at will [see panels (b) and (c)]. The color coding for charge distributions is consistently taken such that red corresponds to negative and blue to positive charge density [in gray scale all shades are to be considered red except for the dark gray regions in panel (d)]. (a) Outline of top gates by showing the charge distribution on these gates. The 1-μm bar shows chosen length scale. (b) Charge distribution in the 2DEG with the center gate at the same voltage as the gates separating the other qubits. (c) Same as (b) but with the voltage on the center gate lifted such that additional charge accumulation is allowed in the 2DEG underneath the gate. (d) Differences in the charge distribution for the setup in (c) resulting from small variations on the plunger gate voltages chosen such that the total change of charge within one dot is $\pm e/2$. (e) Free electrostatic energy of the different charge configurations shown in (d) taken relative to the first configuration No. 1.

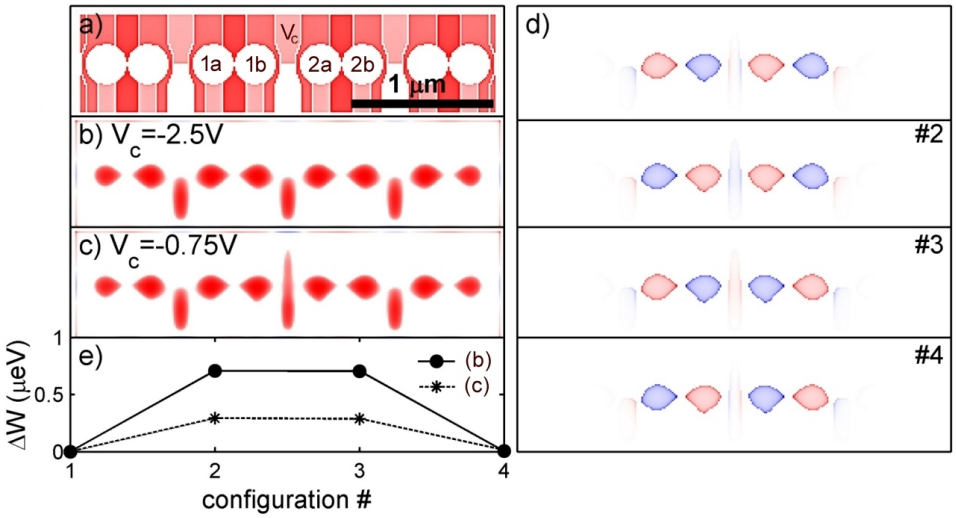

FIG. 4. (Color online) Same as Fig. 3 but with the center gate [labeled V_c in panel (a)] extending only halfway through from top to bottom. This structure has also slightly increased quantum dot spacing and size from that in Fig. 3. The color coding for charge distributions is the same, with red for negative and blue for positive charge density [in gray scale all shades are to be considered red except for the dark gray regions in panel (d)]. See the description of panels (a)–(e) in the caption of Fig. 3.

single dot, then the total difference in charge ΔQ_i for dot i is $|\Delta Q_i| = e/2$ up to numerical precision. Note that the influence on the outer qubits—i.e., the qudot pair on the very left and the very right as seen in panels (b) and (c)—is minimal, and no appreciable charge rearrangement occurs there due to the charge alterations in the two middle qubits.

From the numerical evaluation of the electrostatics, we obtain the potential of the quantum dot array together with the total charge on every dot. For a calculated set of initial values q_a and V_a for the charge and the potential on the individual dots, the electrostatic free energy is evaluated using $\Delta W_{ab} = \int_{q_a}^{q_b} V(q'; V_g) dq'$. The vector V_g stands for a set of external potentials held at constant voltage. For the case of weak changes in the systems electrical geometry, the total change in free energy for different charge configurations is given by[13]

$$\Delta W_{ab} \simeq \Delta q \frac{1}{2}(V_a + V_b), \tag{1}$$

where $\Delta q \equiv q_b - q_a$. For a constant geometry (capacitance matrix) this equation holds exactly. However, in the relevant cases here where gate voltages do change the geometry—namely the shape of the quantum dots as well as the remaining extended regions of charge in the 2DEG—Eq. (1) only holds to first order in small variations of the geometry. Yet this is definitely the case for the single-electron hopping processes considered here.

The qubit-qubit interaction energy for the configurations in panel (d) is then evaluated by means of Eq. (1) with the results shown in panel (e) of Fig. 3. The quantum dots have been intentionally designed not to be exactly the same, resulting in small relative charge variations (maximum deviation of two electrons between the dots). This variation is also reflected in the slight asymmetry seen in panel (e) between the ideally equivalent cases shown in the panels (d). For the setup in panel (b) with the charge depleted under the center gate, the qubit-qubit interaction energy is given by $\Delta E \simeq 1.17$ μeV. By lifting the potential on the center gate from $V_c = -2.4$ V to $V_c = 0$ V, thus allowing extra charge to screen the qubit-qubit interaction [see middle of panel (c)], the interaction energy is reduced to $\Delta E \simeq 0.66$ μeV which is about half the former value.

The quantum dot spacing is about 300 nm from center to center of charge within a qubit and 430 nm between neighboring qubits. Considering the initial half-integer configuration as neutral—i.e., the negatively charged qudots as screened by the environment—then a simple classical estimate of the energy scale for the qubit-qubit interaction by shifting half of an electron charge in between the qubit gives 65 μeV, which is two orders of magnitude larger than the actual realization of dots formed by depletion. This strong suppression of the interqubit interaction is clearly due to the large metallic top gates which efficiently screen the slightly rearranged charge configurations closeby.

A similar calculation was performed with the center gate stretching only halfway through the qubit-qubit intermediate regions. The results are shown in Fig. 4. The average distance between the qudots is slightly different from the previous case (320 nm intraqubit vs 430 nm interqubit separation). The confining potentials on the top gates are slightly weaker, allowing larger dots with about 300 electrons each. The remaining parameters are the same as in the previous case.

The dots are completely symmetric in this case, reflected in the energy of the equivalent charge configurations in panel (d) plotted in panel (e). Again, the qubit-qubit interaction energy for each configuration in panel (d) was evaluated using Eq. (1) and results shown in panel 3(e). For the setup in panel (b) with the charge depleted all along the center gate, the qubit-qubit interaction energy is given by $\Delta E \simeq 0.71$ μeV. By raising the potential on the center gate from

$V_c=-2.5$ V to $V_c=-0.75$ V, the interaction energy is reduced to $\Delta E \simeq 0.29$ μeV which is less than half the former value, but still clearly present. The simple classical estimate similar to the previous example with the extra charge in the qudots positioned around the center of charge leads to 71 μeV, again two orders of magnitude larger than the energies in the actual realization.

IV. CONCLUSIONS

The tunability of qubit interaction based on electrostatic gate screening has been analyzed numerically. Our program uses an efficient relaxation algorithm and efficiently describes general 3D structures, including the ability to handle an extended set of boundary conditions, specifically appropriate for the treatment of 2DEG systems and including dielectric effects.

The typical systems analyzed are based on 2DEG geometries derived from GaAs/GaAlAs structures and depletion via top gates. For a chain of qudot pairs—the qubits—the region in the 2DEG between qubits is depleted at will, allowing for tunable screening and control of the nearest-neighbor qubit interaction. The tunability derived for realistic gate voltage changes is on the order of 50%. The interaction energy can thus be clearly modulated. However, we find that it cannot be turned *off* for moderate voltages, as would be desirable for the on-off switching of the interaction of ideal qubits. We believe that this general trend does not only hold for the few systems analyzed in this paper. The tunability based on charge rearrangement and screening of Coulomb interaction on charged-localized quantum dots is definitely possible, but limited in efficiency. It may indeed be necessary to implement dynamic pulse control techniques, such as the "bang-bang" approach or others discussed for qubits recently.[15]

ACKNOWLEDGMENTS

We acknowledge helpful discussions with T. Ihn and the whole group of K. Ensslin, as well as their hospitality. The work was partially supported by NSF Grant No. NIRT 0103034 and the Condensed Matter and Surface Sciences Program at Ohio University.

APPENDIX: RELAXATION ON THE GRID AND OPEN BOUNDARIES

The algorithm used in this paper is based on a higher-order relaxation algorithm for a finite physical system as described by the authors in an earlier paper.[16] Major modifications are significantly optimized update of the outer boundary and an extended set of additional boundary conditions mainly related to 2DEG systems. As later ones represent dielectric media it is also clear that a proper treatment of surfaces requires a proper incorporation of the dielectric constant. A detailed description can be found in Ref. 13.

Solving the electrostatics in 3D for a finite system with an *open* outer boundary may not allow for a simple boundary condition such as constant potential on the outer surface. With uniform grid spacing, one is bound to a finite total grid size, which in 3D is even more stringent. Therefore the region under investigation cannot assume constant potential on the outer boundary. However, by having direct access to the local charge distribution throughout the grid during relaxation, one can *calculate* the potential on the outer boundary. The naive way of summing up charge over distance $V_i \sim \Sigma_j q_i/d_{ij}$, however, is computationally expensive, to the extent that the actual relaxation process becomes much faster compared than the self-consistent update of the outer boundary.

The reason for this lies in the folding of the charge versus the relative distance. The structure of the sum suggests the use of fast Fourier transform (FFT) algorithms in 3D (Ref. 17) where the folding is replaced by a single product for each Fourier component. The fact that the FFT automatically implies periodic boundary conditions which may introduce artificial effects can be circumvented by doubling the system size in every dimension.[18] Despite the largely enhanced number of grid points in 3D, the resulting update of the outer boundary is drastically two orders of magnitude faster than the original way of carrying out the sum in real space.

Typical materials such as Ga(Al)As or Al_2O_3 have a large dielectric constant of order $\varepsilon=12$. This strongly affects the screening of charges such as those in the 2DEG or surface charges, and it is absolutely crucial to include the dielectric properties in these calculations. The numerical implementation goes along the lines of algorithms found in the literature,[19,20] and it is discussed in detail in Ref. 13. The main idea is that the local relaxation of the potential must be done under the constraint that there be no free charge in the bulk dielectric media. This leads to the incorporation of the dielectric constant into the weights of the potential average over neighboring sites, $V_i^{\text{new}}=\Sigma_{j\in \text{NN}}\epsilon_j q_j/\Sigma_{j\in \text{NN}}\epsilon_j$. One should be aware that the dielectric constant ϵ_j has to be evaluated midway between the grid point i under consideration and the neighboring point j.[13] Finally, note that the subsequent calculation of the source q_i from the potential *without* weighting it by the dielectric constant gives the *induced* charge at dielectric boundaries (note that in uniform dielectric media, the dielectric constant drops out in the averaging process for the local update of V_i^{new} and so the induced charge equals zero by construction).

[1] Andreas Fuhrer, Thomas Ihn, Klaus Ensslin, W. Wegscheider, and M. Bichler, Phys. Rev. Lett. **91**, 206802 (2003).
[2] A. Pioda, S. Kičin, T. Ihn, M. Sigrist, A. Fuhrer, K. Ensslin, A. Weichselbaum, S. E. Ulloa, M. Reinwald, and W. Wegscheider, Phys. Rev. Lett. **93**, 216801 (2004).
[3] T. Hayashi, T. Fujisawa, H. D. Cheong, Y. H. Jeong, and Y. Hirayama, Phys. Rev. Lett. **91**, 226804 (2003).
[4] T. Fujisawa, T. Hayashi, H. D. Cheong, Y. H. Jeong, and Y. Hirayama, Physica E (Amsterdam) **21**, 1046 (2004).
[5] J. Jefferson and W. Häusler, Phys. Rev. B **54**, 4936 (1996).
[6] G. Toth and C. S. Lent, Phys. Rev. A **63**, 052315 (2001).
[7] J. Gorman, D. G. Hasko, and D. A. Williams, Phys. Rev. Lett. **95**, 090502 (2005).
[8] M. Nielsen and I. Chuang, *Quantum Computation and Quantum Information* (Cambridge University Press, Cambridge, England, 2000).
[9] Alex Marchi, Andrea Bertoni, Susanna Reggiani, and Massimo Rudan, Semicond. Sci. Technol. **19**, S415 (2004).
[10] T. Vančura, S. Kičin, T. Ihn, K. Ensslin, M. Bichler, and W. Wegscheider, Appl. Phys. Lett. **83**, 2602 (2003).
[11] L. J. Klein, K. A. Slinker, J. L. Truitt, S. Goswami, K. L. M. Lewis, S. N. Coppersmith, D. W. van der Weide, Mark Friesen, R. H. Blick, D. E. Savage, M. G. Lagally, Charlie Tahan, Robert Joynt, M. A. Eriksson, J. O. Chu, J. A. Ott, and P. M. Mooney, Appl. Phys. Lett. **84**, 4047 (2004).
[12] G. L. Snider, I.-H. Tan, and E. L. Hu, J. Appl. Phys. **68**, 2849 (1990).
[13] A. Weichselbaum, Ph.D. thesis, Ohio University, 2004.
[14] A. Kawaharazuka, T. Saku, C. A. Kikuchi, Y. Horikoshi, and Y. Hirayama, Physica E (Amsterdam) **13**, 663 (2002).
[15] L. Tian and S. Lloyd, Phys. Rev. A **62**, 050301(R) (2000).
[16] Andreas Weichselbaum and Sergio E. Ulloa, Phys. Rev. E **68**, 056707 (2003).
[17] T. Korsmeyer, J. Singer, J. Tausch, J. F. Wang, and J. White (unpublished).
[18] R. Hockney and J. Eastwood, *Computer Simulations Using Particles* (Adam Hilger, Philadelphia, 1988).
[19] M. Davis and J. McCammon, J. Comput. Chem. **12**, 909 (1991).
[20] I. Klapper, R. Hagstrom, R. Fine, K. Sharp, and B. Honig, Proteins: Struct., Funct., Genet. **01**, 47 (1986).